

3D MULTIFRACTAL ANALYSIS: APPLICATION FOR EPILEPSY DETECTION IN SPECT IMAGING

Lopes R.^{1,2}, Makni N.^{1,2}, Viard R.¹, Steinling M.³, Maouche S.², Betrouni N.¹

¹ Inserm, U703
Pavillon Vancostenobel, CHRU Lille
Lille Cedex 59037, France

² LAGIS, CNRS UMR 8146
USTL, Bâtiment P2, Villeneuve d'Ascq, 59655, France

³ Nuclear Medicine Department (SCMN)
University Hospital of Lille, France

ABSTRACT

In medical imaging, many texture analysis methods were studied with different degrees of effectiveness. These last years, works showed the usefulness of the fractal geometry to characterize textures. The fractal dimension provides a global aspect of the texture, while the multifractal analysis provides a local and global aspect of the texture. In this study, we were interested in the detection of epileptic fit sources on brain SPECT images. The detection problem is formulated as a 3D multifractal analysis scheme. The first results obtained on a base of 5 patients show that this method can be effective for this application.

Key Words—3D multifractal analysis, SPECT imaging, epilepsy, detection.

1. INTRODUCTION

During the last years, many works based on texture analysis were applied in medical image analysis [1;2]. Among the most wide-spread tools, the co-occurrence matrix and Haralick parameters [3-5], Fourier spectrum-based methods [6] and the Gabor filter [7;8]. Recently, fractal geometry has emerged as a new texture analysis way. After applications mainly in the discrimination of two states (healthy versus pathological, for example), works enabled to experience of the usefulness of this geometry concerning the texture heterogeneities detection [9;10]. First works concerning this field used the fractal dimension, which enables to take into account the degree of regularity of the organizational structure related to the physical system's behaviour. This method gives only a global view of the surface in general and of the texture in particular. As an improvement, the multifractal analysis was used in medical imaging in various fields, such as the classification [11], the segmentation [12]

and the discrimination between healthy and pathological patient [13].

We are interested here in the multifractal analysis because it enables a local and global study of image irregularities. The multifractal approach was introduced in the 1980s with Mandelbrot multiplicative cascade models of energy dissipation in fully developed turbulence. For image analysis, its application is still restricted to 2D case. By this work, we introduce a 3D model with an application for the epileptic fit sources detection on SPECT images.

2. METHOD

2.1 Theoretical aspect

We start with the following definitions due to Vehelet al.[14], to formulate this approach in 3D.

Definition 1: Let E be a set. A paving on E is a set ε of subsets of E containing the empty set and stable under finite intersection. The pair (E, ε) is called a *paved space*.

We note $P(E)$ the power set of E .

Definition 2: Let (E, ε) be a paved space. A Choquet ε capacity is a function $c: P(E) \rightarrow \mathbb{R}$ with the following properties:

- c is non decreasing: if $A \subset B$, then $c(A) \leq c(B)$.
- If (A_n) is an increasing sequence of subsets of E , i.e.
 $A_n \subseteq A_{n+1}$, then $c\left(\bigcup_n A_n\right) = \sup_n c(A_n)$.
- If (A_n) is a decreasing sequence of elements of ε ,
i.e. $A_{n+1} \subseteq A_n$, then $c\left(\bigcap_n A_n\right) = \inf_n c(A_n)$.

We only consider Choquet capacities defined on $E = [0,1[$, and taking values in $[0,1]$. Let $c = c_{n>1}$ be a sequence of capacities defined on $[0,1[$, and $P = \left(\left(I_j^n \right)_{0 \leq j \leq v_n} \right)_{n \geq 1}$ a sequence of partitions of $[0,1[$. We assume that the following conditions are met:

- $\lim_{n \rightarrow \infty} \max_{0 \leq j \leq v_n} |I_j^n| = 0$.
- For all n, k , I_j^n is a semi open interval.
- For all n, j , $0 \leq j \leq v_n$, there exist k such as $I_j^n \subset I_k^{n-1}$ ($I_j^n \neq I_k^{n-1}$), where $I_0^0 = E(iv)$.
- For all $\alpha > 0$, $\limsup_{I \in P, |I|=0} |\alpha k(I)| \leq 1$, where

$$k(I_j^n) = \sup \left\{ \frac{|I_j^n|}{|I_k^{n+1}|}; I_k^{n+1} \subset I_j^n \right\}.$$

Let,

$$\alpha_n(x) = \frac{\log c_n(I^n(x))}{\log \mu(I^n(x))} \quad (1)$$

Which is defined when $c_n(I^n(x)) \mu(I^n(x)) \neq 0$, and $\alpha(x) = \lim_{n \rightarrow \infty} \alpha_n(x)$ when this limit exists.

This quantity $\alpha_n(x)$ is called *the pointwise Hölder exponent* of c at point x with respect to μ , μ is the Borel measure. In the practical, we define *the local singularity coefficients*, often called *the Hölders coefficients* by:

$$\alpha(x) = \lim_{\delta \rightarrow 0} \frac{\log(\mu(B_\delta(x)))}{\log(\delta)} \quad (2)$$

Where $B_\delta(x)$ is an open-ball of diameter δ centered at the point x .

This quantity reflects the local behaviour of the measure μ around x .

Points bearing the same coefficients can be grouped into sets, named *iso-local singularity sets*, defined by:

$$E(\alpha) = \{x : \alpha(x) = \alpha\} \quad (3)$$

We can define above these sets with ε threshold value as follow:

$$E_\varepsilon(\alpha) = \{x : \alpha - \varepsilon \leq \alpha(x) \leq \alpha + \varepsilon\} \quad (4)$$

To characterize the above sets, we define set dimensions known as the *Hausdorff dimension*:

$$\dim_H E = \sup \left\{ s : \liminf_{\delta \rightarrow 0} \sum_{i=0}^{\infty} |E_i|^s = 0 \right\}$$

$$= \sup \left\{ s : \liminf_{\delta \rightarrow 0} \sum_{i=0}^{\infty} |E_i|^s = \infty \right\} \quad (5)$$

Where $\{E_i\}_{1 \leq i \leq \infty}$ is an δ cover of E . $E \subset \bigcup_{i=0}^{\infty} E_i$, $|E_i| < \delta$,

$E_i \subset P$ for all i .

Finally, we define:

$$f(\alpha) = \dim_H E(\alpha) \quad (6)$$

The description $(\alpha, f_h(\alpha))$ is called *the local singularity spectrum* or *the Hausdorff spectrum (Hölder)* of the multifractal measure μ .

2.2 Implementation

Since the Hausdorff dimension can not be evaluated directly, we use discretization of the above concepts of capacities and measures. Equation (2) is computed as follow:

Points x are associated to voxels of 3D signal. We subdivide the signal by δ -size cube centered at voxels, rather than open-balls.

We define the measure μ as the sum of the grey level intensities of voxels (i,j,k) contained in a cube centered at the voxel (x,y,z) .

Let $g(x,y,z)$ denote the grey level at (x,y,z) .

$$\mu_{\text{sum}}(x,y,z) = \sum_{(i,j,k) \in B_\delta(x,y,z)} g(i,j,k) \quad (7)$$

This measure represents two distributions, to known the spatial and sharpness distribution.

Other types of measures can be defined, « max » and « min » capacities represent the sharpness of the image in the neighbourhood of the voxel (x,y,z) . They are called *altimetric capacities*.

$$\mu_{\text{max}}(x,y,z) = \max_{(i,j,k) \in B_\delta(x,y,z)} g(i,j,k) \quad (8)$$

$$\mu_{\text{min}}(x,y,z) = \frac{1}{\max_{(i,j,k) \in B_\delta(x,y,z)} g(i,j,k)} \quad (9)$$

The last step in the evaluation of Hölders coefficients is to replace the limit of the equation (2) by the slope of the least squares linear fit to the log-log graph of δ vs μ .

Once Hölders coefficients obtained, we establish iso-local singularity sets $E(\alpha)$ using equation (4). The threshold value ε of the equation is assimilated at discretization step of an interval. Indeed the set $[\alpha_{\min}, \alpha_{\max}]$ is discretized in N subsets of size ε .

Finally, $f(\alpha)$ (named the singularity spectrum) is defined as the fractal dimension of the set $E(\alpha)$, which has a monofractal structure. Consequently we estimate $f(\alpha)$ by the box-counting method extended in 3D.

Patients	Expert diagnostic	Results of our method		
N°	Temporal lobe	Temporal lobe?		
		Min	Max	Sum
1	Left	Left	Left	Left
2	Left	Left	Left	Left
3	Left	Left	?	Left
4	Left	Left	Left	Left
5	Right	Right	?	?
6	Right	Right	Right	Right
7	Right	Right	Right	Right

Table 1. Comparison of results between our method and the expert diagnostic. Display the localization of the seizure in the lobe temporal (left or right) (? = indeterminate).

4. RESULTS

In a previous study [15], we generated self-affine and self-similar multifractal models to validate these measures. The multifractal spectrum of each measure was a very good approximation of the theoretical spectrum.

3. APPLICATION

Epilepsy is a neurological disease. It is the expression of an abnormal, sharp and temporary functioning of the brain electrical activity, leading epileptic crisis, also called comitial crisis. Two exams can be executed for the diagnostic, the electroencephalogram (EEG) and SPECT imaging. For this last case, two acquisitions are carried out: an examination before the crisis called inter-ictal exam and another after the crisis, called per-ictal. To analyse the images, these two exams are rigidly registered to eliminate movements between the two steps then subtracted to determinate the regions responsible of the crisis. Usually, for a better localization, the result of the subtraction is matched with anatomical data providing from magnetic resonance imaging (MRI). This technique is called SISCOM (Substracted Ictal Spect COrregistred to MRI) [16]. However, in some cases and for many reasons, the method does not lead to precise delimitation of epileptic fit sources. We apply the 3D multifractal analysis method described in section 2 to characterize epileptic fit sources. For the epileptic patient, there is heterogeneity changing between the two exams. Indeed the per-ictal sequence represents the patient in crisis, whereas the inter-ictal sequence represents the brain activity in a rest candition. Consequently we decide to study the heterogeneity changes between the two conditions using the singularity spectrum. We compute the local singularity spectrum of each voxel of inter and per-ictal volumes, for three various multifractal measures (« sum », « max » and « min ») then we subtract these two volumes to give only the important heterogeneity change area. Finally a connex component study is used to remove isolated points.

We tested the method on brain SPECT images provided by the Nuclear medicine centre of Lille. Tc-99m HMPAO brain perfusion ictal and interictal images were acquired on a Tomomatic 564 (Medimatic Inc., Copenhagen, Denmark). Thus we have two volumes $64*64*18$ voxels ($3.25*3.25*6.5$ mm³). The patient base contains 7 patients diagnosed as epileptic (partial seizure). The seizure is localised in the temporal lobe. This diagnostic was realized by an expert.

We apply our method on this patient base. The singularity spectrum is computed for the three various measures (« sum », « max » and « min »). The most interesting results are obtained with the « min » measure. Indeed, the table 1 displays results obtained for each measure, we can see that the “min” measure is totally in agree with the expert diagnostic, while the “max” and “sum” measure don’t always detect the seizure. Therefore we display results obtained by the “min” measure. The figure 1 represents results obtained by the method on two patients, they are displayed according to three directions (transversal, coronal and sagittal) for a best localization of epileptic fit sources. The uni-lateral epilepsy character was verified by the method, according to the expert diagnostic. Indeed for the five patients, we found a left or right localization of the seizure, which agrees with the expert diagnostic.

5. CONCLUSION AND FUTURE WORK

In this paper, we presented a method for the 3D local singularity spectrum evaluation. It is applied on SPECT images in order to detect the epileptic fit sources. The preliminary results are encouraging and prove that this kind of analysis can be effective.

As future work, we plan to test the method on frontal epilepsy images. Indeed, in addition to enlarge our image base, for this kind of epilepsies, the crisis is often less accentuated and therefore experts don’t always permit to

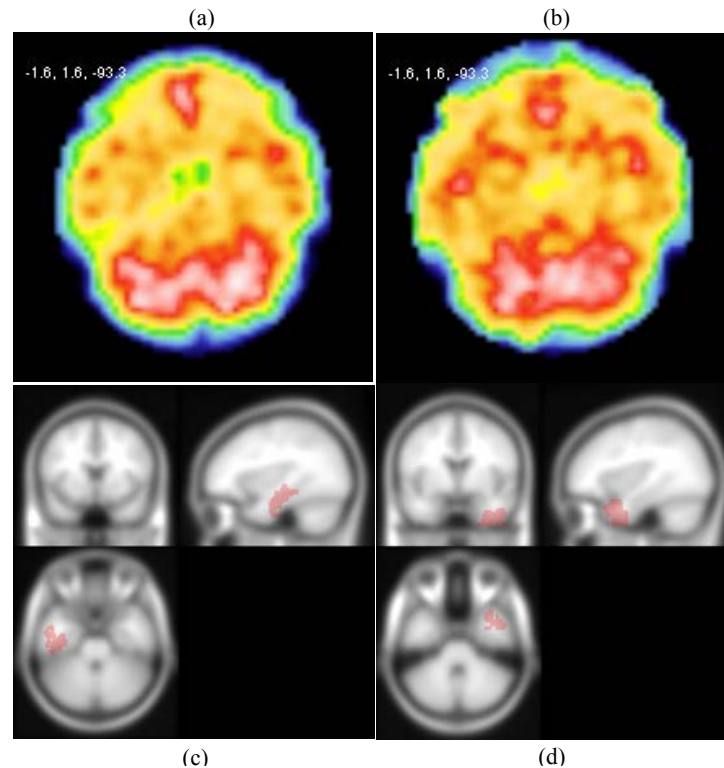


Figure 1: Display inter-ictal (a) and per-ictal (b) images for one patient. Result of the method for two patients, the one with an epilepsy at left temporal lobe (c) and the other at right temporal lobe (d). Display following three directions (transversal, coronal and sagittal) on the MNI atlas.

localize the epileptic fit sources. Thus, it is interesting to quantify the contribution of such a tool. The expert could

limit the epileptic fit sources, so we could have statistical results. Finally, we envisage to add various texture parameters (co-occurrence matrix, Gabor filter, etc.) to improve the detection.

6. REFERENCES

- [1] V. Kovalev, F. Kruggel, H. Gertz, and D. Cramon, "Three-dimensional texture analysis of MRI brain datasets," *IEEE Transactions on Medical Imaging*, vol. 20, no. 5, pp. 424-433, 2001.
- [2] A. Madabhushi, M. Feldman, D. Metaxas, J. Tomaszewski, and D. Chute, "Automated detection of prostatic adenocarcinoma from high-resolution ex vivo MRI," *IEEE Transactions on Medical Imaging*, vol. 24, no. 12, pp. 1611-1625, 2005.
- [3] O. Basset, Z. Sun, J. Mestas, and G. Gimenez, "Texture analysis of ultrasonic images of the prostate by means of co-occurrence matrix," *Ultrason. Imag.*, vol. 15, no. 218, p. 237, 1993.
- [4] R. Haralick, K. Shanmugan, and I. Dinstein, "Textural features for image classification," *IEEE Trans. Syst. Man, Cybern.*, vol. SMC-3, pp. 610-621, 1973.
- [5] W. Chen, M. Giger, H. Li, U. Bick, and G. Newstead, "Volumetric texture analysis of breast lesions on contrast-enhanced magnetic resonance images," *Magnetic Resonance in Medicine*, vol. 58, no. 3, pp. 562-571, 2007.
- [6] R. Brown, H. Zhu, and J. Mitchell, "Distributed vector processing of a new local multi-scale fourier transform for medical imaging applications," *IEEE Transactions on Medical Imaging*, vol. 24, no. 5, pp. 689-691, 2005.
- [7] Pitiot, A. Toga, N. Ayache, and P. Thompson, "Texture based MRI segmentation with a two-stage hybrid neural classifier," *Proceedings of the 2002 International Joint Conference on Neural Networks*, vol. 3, pp. 2053-2058, 2002.
- [8] Q. Zhen, A. Montillo, D. Metaxas, and L. Axel, "Segmenting cardiac MRI tagging lines using Gabor filter banks," *Proceedings of the 25th Annual International Conference of the IEEE*, vol. 1, pp. 630-633, 2003.
- [9] C. Chen, J. DaPonte, and M. Fox, "Fractal feature analysis and classification in medical imaging," *IEEE Transactions on Medical Imaging*, vol. 8, no. 2, pp. 133-142, 1989.
- [10] D. Chen, R. Chang, C. Chen, M. Ho, S. Kuo, S. Hung, and W. Moon, "Classification of breast ultrasound images using fractal feature," *Clinical Imaging*, vol. 29, no. 4, pp. 235-245, 2005.
- [11] P. Kestener, J. Lina, P. Saint-Jean, and A. Arneodo, "Wavelet-based multifractal formalism to assist in diagnosis in digitized mammograms," *Image Anal Stereol*, vol. 20, no. 3, pp. 169-175, Aug.2004.
- [12] Y. Xia, D. Feng, and R. Zhao, "Morphology-based multifractal estimation for texture segmentation," *IEEE Trans. Image Process*, vol. 15, no. 3, pp. 614-623, Mar.2006.
- [13] T. Stosic and B. D. Stosic, "Multifractal analysis of human retinal vessels," *IEEE Trans. Med. Imaging*, vol. 25, no. 8, pp. 1101-1107, Aug.2006.
- [14] J. Vehel and R. Vojak, "Multifractal analysis of Choquet capacities," *Advances in applied mathematics*, vol. 20, no. 1, pp. 1-43, 1998.
- [15] R. Lopes, P. Dubois, I. Bhouri, P. Puech, S. Maouche, and N. Betrouni, "Multidimensional models for methodological validation in multifractal analysis," *Conf. Proc. IEEE Eng Med. Biol. Soc.*, vol. 1, pp. 5543-5546, 2007.
- [16] T. O'Brien, E. So, B. Mullan, M. Hauser, B. Brinkmann, N. Bohnen, D. Hanson, G. Cascino, C. Jr. Jack, and F. Sharbrough, "Subtraction ictal SPECT co-registered to MRI improves clinical usefulness of SPECT in localizing the surgical seizure focus," *Neurology*, vol. 50, pp. 445-454, 1998.